J Mater Sci (2008) 43:5508–5515
DOI 10.1007/s10853-008-2832-6

Prediction of metadynamic softening in a multi-pass hot deformed low alloy steel using artificial neural network

Y. C. Lin · Xiaoling Fang · Y. P. Wang

Received: 12 March 2008 / Accepted: 24 June 2008 / Published online: 15 July 2008

Abstract The metadynamic softening behaviors in 42CrMo steel were investigated by isothermal interrupted hot compression tests. Based on the experimental results, an efficient artificial neural network (ANN) model was developed to predict the flow stress and metadynamic softening fractions. The effects of deformation parameters on metadynamic softening behaviors in the hot deformed 42CrMo steel have been investigated by the experimental and predicted results from the developed ANN model. Results show that the effects of deformation parameters, such as strain rate and deformation temperature, on the softening fractions of metadynamic recrystallization are significant. However, the strain (beyond the peak strain) has little influence. A very good correlation between experimental and predicted results indicates that the excellent capability of the developed ANN model to predict the flow stress level and metadynamic softening, the metadynamic recrystallization behaviors were well evidenced.

Y. C. Lin (✉)
Key Laboratory of Modern Complex Equipment Design and Extreme Manufacturing of the Ministry of Education, School of Mechanical and Electrical Engineering, Central South University, Changsha 410083, China
e-mail: yclin@mail.csu.edu.cn; linyongcheng@163.com

X. Fang
Department of Chemical and Petroleum Engineering, Karamay Vocational & Technical College, Xinjiang 833600, China

Y. P. Wang
School of Chemical Engineering, Inner Mongolia Polytechnic University, Huhhot 010062, China

Introduction

The hot rolling and forging processes often consist of several successive deformation stages, including inter-pass periods between deformations. During the inter-pass periods, the metals and alloys will subject the dynamic recovery, static recrystallization, and metadynamic recrystallization. Meanwhile, the materials are often subjected to complex time, strain, strain rate, and temperature histories in industrial forming processes. On the one hand, a given combination of thermo-mechanical parameters yields a particular metallurgical phenomenon, including the microstructural evolution during the inter-pass periods; on the other hand, microstructural changes of the metal in turn affect the mechanical characteristics of the metal such as the flow stress, and hence influence the forming process. Therefore, the constitutive flow behaviors of materials, especially in multi-stage or multi-pass processing, are quite complex in nature [1–7].

The conventional methods are to carry out the regression analysis with the experimental results on the basis of the classical models to obtain the constants in the models. However, the response of the deformation behaviors of the materials under elevated temperatures and strain rates is highly nonlinear, and many factors affecting the flow stress are also nonlinear, which make the accuracy of the flow stress predicted by the regression methods low and the applicable range limited [8–11]. However, the field of neural networks can be thought of as being related to artificial intelligence, machine learning, parallel processing, statistics, and other fields. The attraction of artificial neural networks (ANN) is that they are best suited to solving the problems that are the most difficult to solve by traditional computational methods. Neural networks can provide a fundamentally different approach to materials modeling and material processing control techniques than

statistical or numerical methods. One of the main advantages of this approach is that it is not necessary to postulate a mathematical model at first or identify its parameters using a neural network. In the past, some efforts have been made to the applications of neural networks in industry or academic study [12–20].

42CrMo (American grade: AISI 4140) is one of the representative medium carbon and low alloy steels. Due to its good balance of strength, toughness, and wear resistance, 42CrMo high-strength steel is widely used for many general purpose parts including automotive crankshaft, rams, spindles, etc. In the past, many investigations have been carried out on the behavior of 42CrMo steel [7–9, 20–26]. Despite large amount of efforts invested into the behaviors of 42CrMo steel, the kinetics of metadynamic recrystallization in the hot deformed 42CrMo steel still need to be further investigated to study the workability and optimize the hot forming processing parameters.

In this study, the metadynamic softening behaviors in 42CrMo steel were investigated by isothermal interrupted hot compression tests. An efficient ANN model was developed to predict the metadynamic softening fractions and investigate the effects of deformation parameters on metadynamic softening behaviors in the hot deformed 42CrMo steel. Comparisons between the experimental and predicted results were conducted.

Experiments

A commercial 42CrMo high-strength steel of compositions (wt.%) 0.450C–0.280Si–0.960Cr–0.630Mn–0.190Mo–0.016P–0.012S–0.014Cu–(bal.)Fe was used in this investigation. Cylindrical specimens were machined with a diameter of 10 mm and a height of 12 mm. In order to minimize the frictions between the specimens and die during hot deformation, the flat ends of the specimen were recessed to a depth of 0.1 mm deep to entrap the lubricant of graphite mixed with machine oil. In order to study the progress of metadynamic softening, two-pass hot compression tests were performed on a computer-controlled Gleeble-1500 thermo-simulation machine. The specimen is resistance heated by thermo coupled-feedback-controlled AC current.

As shown in Fig. 1, the specimens were heated to 1200 °C at a heating rate of 10 °C/s, held for 5 min and cooled at 10 °C/s to the deformation temperature, held for 1 min to eliminate thermal gradients. Four different deformation temperatures (850, 950, 1050, and 1150 °C) and four different strain rates (0.01, 0.1, 0.5, and 1 s^{-1}) were used in double hit hot compression tests. In order to investigate the effects of strain on the metadynamic recrystallization behavior, three different deformation degrees (a reduction of 30, 40, and 50% in specimen height) were applied. Of course,

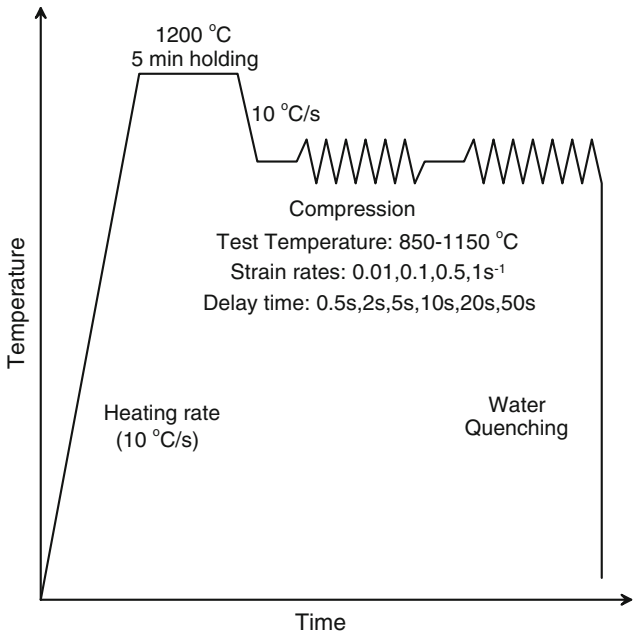

Fig. 1 Experimental procedure for two-pass hot compression tests

the first deformation should be interrupted above the critical strain required for dynamic recrystallization in order to initiate dynamic recrystallization. Then the metadynamic recrystallization would occur in the unloading period (inter-pass). The critical strains had been reported elsewhere [7–9]. The deformation temperatures, strain rates, and the deformation degrees are same for the first and second deformations. After unloading (the phases between the first and second deformations), the specimens were held at the deformation temperature for the inter-pass delay time of 1–50 s to enable metadynamic recrystallization to progress. A second deformation was then applied to measure the amount of softening, and then the specimens were rapidly quenched in water.

Figure 2 shows the typical true stress–strain curves obtained from two-pass hot compression tests of 42CrMo steel for different inter-pass delay time (under deformation temperature of 1050 °C, strain rate of 0.01 s^{-1}, and deformation degree of 30%). It can be found that the yield stress of the second deformation generally decreases as the inter-pass delay time is increased under the same heat treatment history and deformation schedule. The metadynamic softening increase as the delay time is increased. Significant metadynamic recrystallization will occur in the unloading period (inter-pass) when the delay time is increased, which will cause more work hardening in the second deformation. Because the dynamic recrystallization will lead to more fine grain, the grain boundary area per unit volume will increase and in turn accelerate the recrystallization nucleation rate. This will greatly reduce

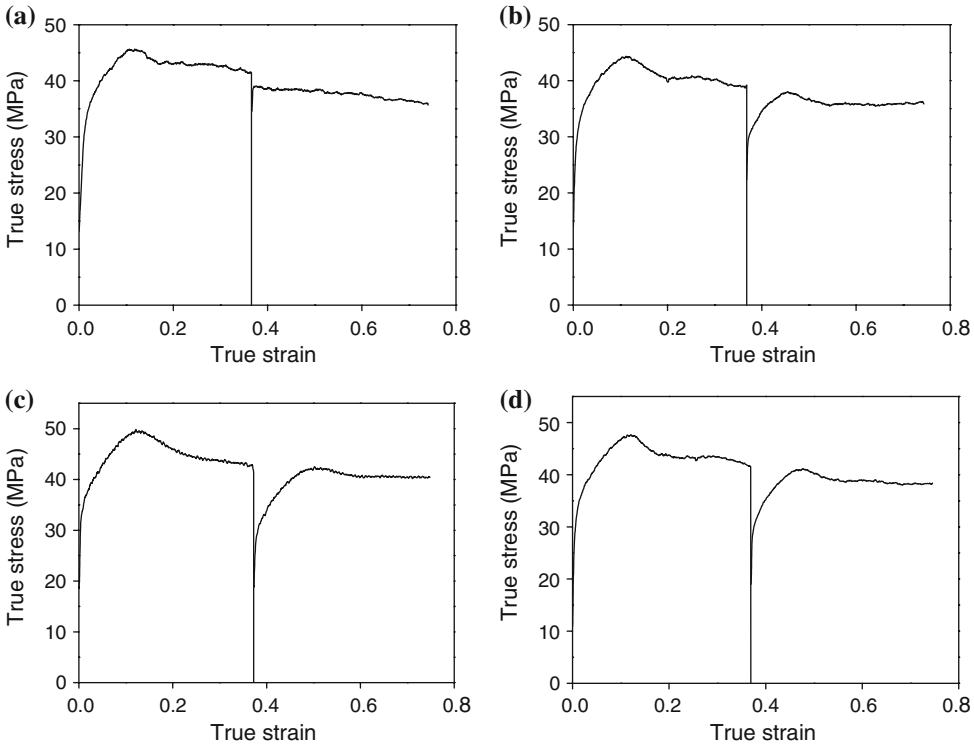

Fig. 2 Typical true stress–strain curves for inter-pass delay time of (**a**) 0.5 s, (**b**) 10 s, (**c**) 20 s, and (**d**) 50 s (under deformation temperature of 1050 °C, strain rate of 0.01 s^{-1}, and deformation degree of 30%)

the peak stress and strain after metadynamic recrystallization. Similar results were obtained under other test conditions.

Development of ANN model for flow stress prediction

Theory of ANN

ANNs are a large class of parallel processing architectures, which can mimic complex and nonlinear relationships through the application of many non-linear processing units called neurons. The relationship can be 'learned' by a neural network through adequate training from the experimental data. It can not only make decisions based on incomplete and disorderly information, but can also generalize rules from those cases on which it was trained and apply these rules to new cases. Usually, the structure of an ANN is hierarchical with neurons grouped in different layers designed as an input layer, hidden layers and on output layer, as shown in Fig. 3. More detailed information about ANN can be found in Ref. [27], which introduced

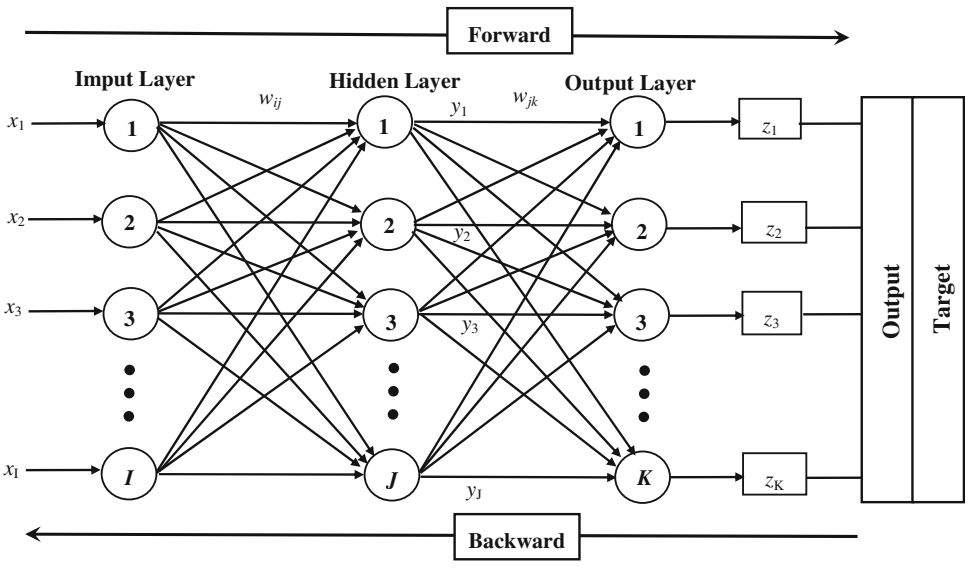

Fig. 3 Schematic structure of the BP neural network

neural networks and reviewed some applications of the technique in the context of materials science.

The multilayer feed forward network with back propagation (BP) learning is the most popular of all ANN models. The feed forward BP neural network is actually composed of two neural network algorithms: (a) feed forward and (b) BP. The term 'feed forward' refers to a method by which a neural network processes the pattern and recalls patterns, whereas the term 'back propagation' describes how this type of neural network is trained. BP is a form of supervised training. When using a supervised training method the network must be provided with sample inputs and anticipated outputs (target), as shown in Fig. 3. These anticipated outputs will be compared against the predicted outputs from the neural network. Then, the BP training algorithm takes a calculated error and adjusts the weights of the various layers backwards from the output layer all the way back to the input layer until a good match is achieved, i.e., the error between the predicted and measured flow stresses is minimized to below a predefined convergence limit. In order to validate the generalization capability of the newly trained ANN, a set of test data, i.e., data not used in the training stage, is supplied as the inputs. If the error between the predicted and anticipated values of output is small enough, the network is well trained. Here, the convergence criterion for the network is determined by the average root mean square (RMS) error between the desired and predicted output values,

$$E_{\mathrm{RMS}} = \frac{1}{N}\sum_{i=1}^{N}\sqrt{\frac{1}{p}\sum_{j=1}^{p}(d_{ji}-y_{ji})^2} \quad (1)$$

where E_{RMS} is the average RMS, N is the number of training or testing data, p is the number of variables in the output, $d_j(n)$ and $y_j(n)$ are the target output and network output for neuron j, respectively. 1% RMS error has been set as the convergence criterion in the ANN model for the flow stress prediction.

Unification of the training set

ANN requires that the range of both input data and output data should be 0–1; consequently, the data must be unified. The widely used method of unification is

$$X_i = 0.1 + 0.8 \times \left(\frac{X - X_{\min}}{X_{\max} - X_{\min}}\right) \quad (2)$$

where X is the original data, $X_{\min}$ the minimum value of X, $X_{\max}$ the maximum value of X, and X_i the unified data of the corresponding X. It should be emphasized that the logarithmic value of strain rate ($\dot{\varepsilon}$) was used in present study because $\dot{\varepsilon}$ changes severely and causes too small a unified value of $\dot{\varepsilon}_{\max}$ for the ANN to learn.

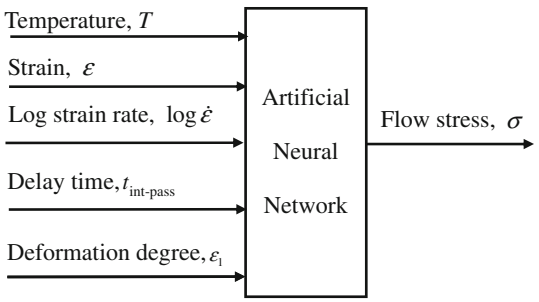

Fig. 4 Schematic of the ANN structure for flow stress prediction for 42CrMo steel

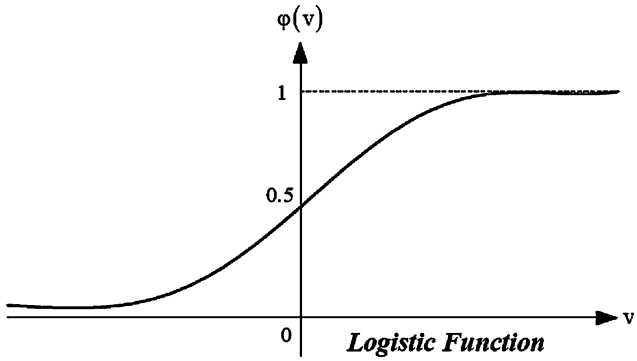

Fig. 5 Shape of logistic sigmoid function

Table 1 Statistical analysis of the variables used to develop the neural network model

Variables	Minimum value	Maximum value	Average	Standard deviation
T, °C	850	1150	1000	129.1
$\dot{\varepsilon}$, s^{-1}	0.01	1	0.40	0.45
ε	0.1	0.9	0.50	0.24
ε_1	0.1	0.7	0.40	0.18
$t_{\text{int-pass}}$	0.5	50	15	19

Design and training of ANN model for flow stress prediction

The schematic of the ANN structure for flow stress prediction in 42CrMo steel is shown Fig. 4. The inputs of the model are strain (ε), log strain rate ($\log\dot{\varepsilon}$), temperature (T), inter-pass delay time ($t_{\text{int-pass}}$), and deformation degree in the first deformation (ε_1). The output of the model is flow stress (σ). The feed forward network with BP learning algorithm has been used to train the model. The learning is based on gradient descent algorithm and hence requires the activation function to be differentiable, and a logistic sigmoid function was employed as the activation function, as shown in Fig. 5.

A total of 600 input/output data points have been selected from 40 stress–strain curves, which were obtained

Table 2 Statistic analysis of the performance of ANN model for training and testing predictions

Learning rate	Weight initialization	RMS error (%)		*R*		AARE (%)		SI	
		Training	Testing	Training	Testing	Training	Testing	Training	Testing
0.1	±0.1	5.78	6.32	0.995	0.993	5.45	4.86	0.052	0.048

from the thermo-simulation experiments. The statistical analysis of the variables (ε, $\log\dot{\varepsilon}$, T, ε_1, $t_{\text{int-pass}}$) used to develop the neural network model for 42CrMo steel is shown in Table 1. All datasets were unified between 0 and 1 in order to ensure that each variable lies in the same range during training and testing. Among these datasets, 70% of the datasets was randomly selected to train the ANN model, while the remainder 30% (previously unused data) was used to test the predictability of the newly trained ANN, that is, to validate the ability of developed ANN model to predict the flow stress for 42CrMo steel. Generally, this iterative process is considered as the appropriate compromise between predictability and overfitting. Additionally, the Bayesian regularization algorithm is combined with BP neural network to obtain the better generalization and faster speed of convergence, and higher learning accuracy because multiple parameters and larger patterns were inputted.

Results and discussion

Neural network results

After repeated trials by changing the number of neurons in the hidden layer from 4 to 30, it was found that a network with one hidden layer consisting of 18 hidden neurons gives a minimum RMS error and thereby considered as the optimal configuration for the prediction of flow stress for 42CrMo steel. The number of iteration is 20,000. In this study, correlation coefficient (R), scatter index (SI), and average absolute relative error (AARE) were used to qualify the generalization capability of the training and testing network, and the expressions of R, SI, and AARE can be written as

$$R = \frac{\sum_{i=1}^{N}(E_i - \bar{E})(P_i - \bar{P})}{\sqrt{\sum_{i=1}^{N}(E_i - \bar{E})^2 \sum_{i=1}^{N}(P_i - \bar{P})^2}} \tag{3}$$

$$\text{AARE}(\%) = \frac{1}{N}\sum_{i=1}^{N}\left|\frac{E_i - P_i}{E_i}\right| \times 100 \tag{4}$$

$$\text{SI} = \frac{E_{\text{RMS}}}{\bar{E}} \tag{5}$$

where E is the experimental result and P is the predicted value obtained from the neural network model. $\bar{E}$ and $\bar{P}$ are the mean values of E and P, respectively. N is the total number of data employed in the investigation. Table 2 shows the performance of neural network predictions for both the training and testing data. It can be found that the values of AARE for the training and test dataset are only 5.45 and 4.86%, respectively, which shows that the generalization capability of the training and testing network is satisfied. Meanwhile, the comparisons between the experimental and corresponding predicted results for both the training and testing datasets of 42CrMo steel are shown in Fig. 6. The trendline involved in Fig. 6 indicates close agreement between the predicted and experimental flow stresses. The results show that a very good correlation between experimental and predicted results has been obtained, which suggests that the neural network is able to successfully predict the compressive deformation behaviors of 42CrMo steel.

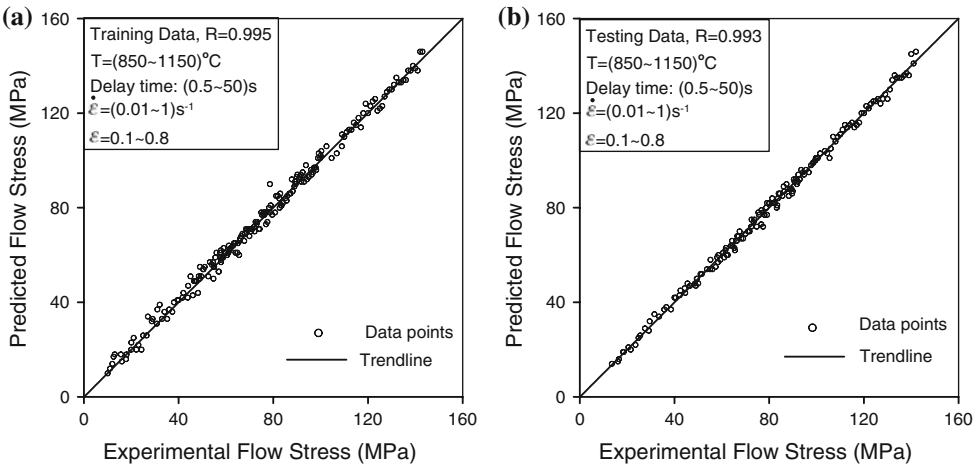

Fig. 6 Comparisons between the experimental and predicted flow stress of 42CrMo steel using the BP ANN model: (**a**) predicted training data and (**b**) predicted testing data

Application of the developed ANN model to predict metadynamic softening fractions

Metadynamic softening fractions

The interrupted deformation method is based on the principle that the yield stress at high temperatures is a sensitive measure of the structural changes. In this study, the 0.2% offset yield strength was used to determine the softening due to metadynamic recrystallization and recovery. The softening fraction, F_{md}, is determined by the "offset method"

$$F_{md} = \frac{\sigma_m - \sigma_2}{\sigma_m - \sigma_1} \quad (6)$$

where σ_m is the flow stress at the interruption, σ_1 and σ_2 are the offset stress (0.2%) at the first deformation and the second deformation, respectively. σ_m, σ_1, and σ_2 are obtained from the predicted stress–strain curves by the above-developed ANN model.

Influence of deformation parameters on metadynamic softening

The effects of deformation parameters, including the deformation temperature, strain rate, deformation degree, and initial grain sizes, on the metadynamic recrystallization of two-pass hot compressed 42CrMo steel were discussed. Figure 7 shows the relative importance of processing parameters for metadynamic softening predictions. It is obvious that the effects of the deformation temperature and strain rate are significant, while the deformation degree (in the first stage of deformation) affects only slightly. The effects of processing parameters on the metadynamic softening are discussed below. Additionally, it should be pointed out that the experimental data considered in Figs. 8–10 have not been included in the training process of the developed model in order to build an efficient ANN model. In Figs. 8–10, only the mean values of the predictions were given.

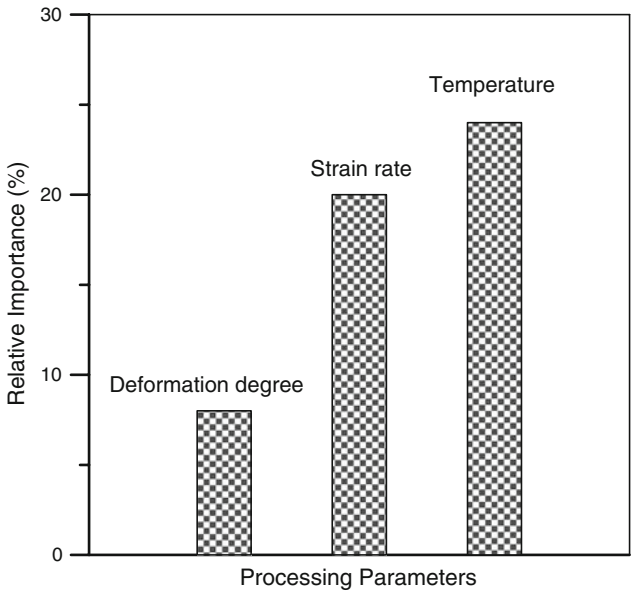

Fig. 7 Bar plots showing the relative importance of processing parameters for metadynamic softening predictions

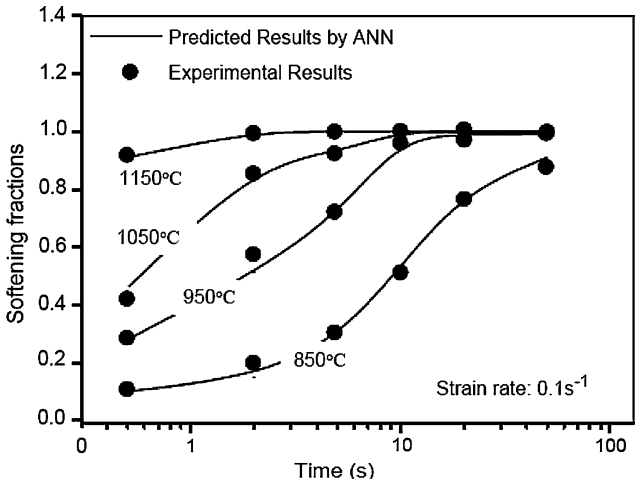

Fig. 8 Effects of deformation temperatures on metadynamic softening

Effects of deformation temperature The metadynamic softening fractions were plotted against the inter-pass delay time for four different deformation temperatures at strain rate of 0.1 s^{-1} and deformation degree of 30%, as shown in Fig. 8. It is obvious that a good agreement between the experimental and predicted results by the developed ANN model is obtained. Figure 8 indicates that the effects of deformation temperatures on metadynamic softening are significant. The softening fractions increase with the

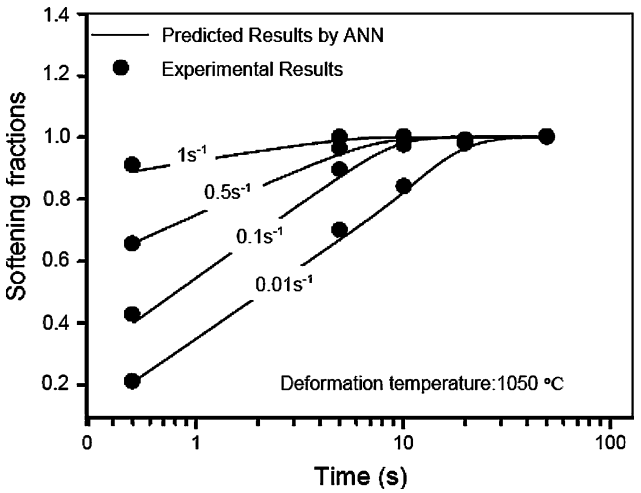

Fig. 9 Effect of strain rates on metadynamic softening

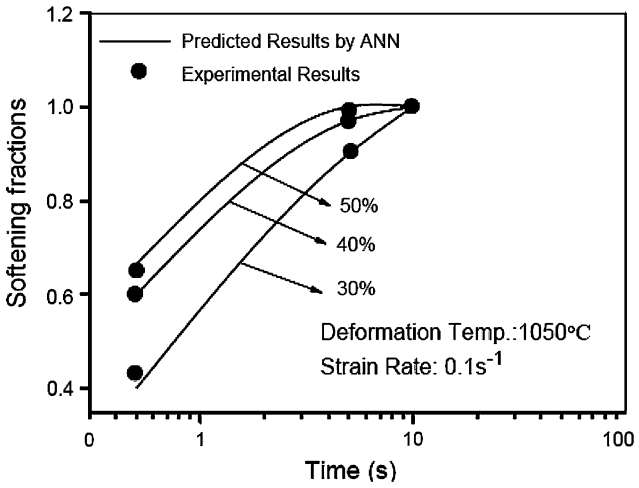

Fig. 10 Effect of deformation degree on metadynamic softening

increase of the deformation temperatures, and the softening curves under deformation temperatures of 850, 950, and 1050 °C follow Avrami equation, i.e., they have conventional sigmoidal appearance. However, under the deformation temperature of 1150 °C, the softening curve appears relatively flat and the values of softening fractions are higher than other deformation temperature conditions, which is induced by the rapid metadynamic recrystallization under high temperature. Meanwhile, under the deformation temperature of 850 °C and the inter-pass delay time of 50 s, the value of softening fraction is only 0.87 and the rate of softening rapidly decreases, which means this test condition cannot result in a complete metadynamic recrystallization. As the softening mechanisms are thermally activated, the fractional softening increases as the temperature increases.

Effects of strain rate Figure 9 shows the changes of softening fractions with inter-pass delay time under different strain rates (under the deformation temperature of 1050 °C and deformation degree of 30%). It is obvious that the predicted results by ANN model are consistent with the experimental ones. Figure 9 indicates that strain rate has a great influence on the fractional softening of metadynamic recrystallization, and it is evident that the recrystallization kinetics is accelerated significantly when the strain rate is increased. The softening fractions with the strain rate of 1 s^{-1} are greatly larger than those with lower strain rates of 0.01 s^{-1}, especially in the shorter inter-pass delay time cases. This is due to the higher strain energy stored in the deformation block under high strain rate conditions as a consequence of lesser time being available for dynamic recovery. Then, the reduced extent of dynamic recovery occurring at higher strain rates in turn produces a higher dislocation density and increases the driving force for recrystallization.

Effects of deformation degree In order to investigate the effect of deformation degree on the kinetics of metadynamic recrystallization of 42CrMo steel, the pre-strain of the first deformation in the double deformation test was varied from the peak strain to the strain at steady state stress, i.e., above the critical strain required for dynamic recrystallization. The critical strain is often taken as about 0.8 ε_p (ε_p is the peak strain) [7–9]. The softening fractions as a function of inter-pass delay time for three pre-strain conditions (a reduction of 30, 40, and 50% of specimen height in the first deformation) are shown in Fig. 10. Both the results of ANN model and experiments indicate that the softening fractions and the rate of softening increase as the deformation degree is increased. The softening curves indicate that strain has little influence upon the softening fractions of metadynamic recrystallization. For dynamic recrystallization, beyond the peak strain, changes in strain do not significantly change the substructure; hence the lack of influence of strain on the metadynamic characteristics. However, for the case of the deformation degree of 30%, it seems that the strain has a little influence upon the softening fractions of metadynamic recrystallization. This attributes to the relatively small pre-strain, which is very close to the critical strain required for dynamic recrystallization.

Conclusion

In this study, a feed forward BP ANN model is developed to predict the flow stress and metadynamic softening of hot deformed 42CrMo steel based on the isothermal interrupted hot compression tests. A very good correlation between experimental and predicted results from the developed ANN model has been obtained, which indicates the excellent capability of the developed ANN model to predict the flow stress level and metadynamic softening of multi-pass hot deformed 42CrMo steel. The effects of deformation parameters on metadynamic softening in the hot deformed 42CrMo steel have been discussed in detail. Both the experimental and predicted results indicate that the effects of deformation parameters, including the strain rate and deformation temperature, on the metadynamic softening in two-pass hot deformed 42CrMo steel are significant. The softening fractions rapidly increase with the increase of the deformation temperatures and/or strain rates, while the effects of deformation degree on the softening are not very marked, which means that pre-strain (the deformation degree of the first compression), beyond the peak strain, has little influence on the softening fraction induced by the metadynamic recrystallization of 42CrMo steel.

Acknowledgement This work was supported by 973 Program (grant no. 2006CB705401), China Postdoctoral Science Foundation

(grant no. 20070410302), the Postdoctoral Science Foundation of Central South University.

References

1. Salehi AR, Serajzadeh S, Taheri AK (2006) J Mater Sci 41:1917. doi:10.1007/s10853-006-4486-6
2. Roy RK, Kar S, Das K, Das S (2006) J Mater Sci 41:1039. doi:10.1007/s10853-005-2226-y
3. Elwazri AM, Essadiqi E, Yue S (2004) ISIJ Int 44:744. doi:10.2355/isijinternational.44.744
4. Fernández AI, Uranga P, López B, Rodriguez-Ibabe JM (2000) ISIJ Int 40:893. doi:10.2355/isijinternational.40.893
5. Di Schino A, Kenny JM, Abbruzzese G (2002) J Mater Sci 37:5291. doi:10.1023/A:1021068806598
6. Morris DG, Gutierrez-Urrutia I, Muñoz-Morris MA (2007) J Mater Sci 42:1439. doi:10.1007/s10853-006-0564-z
7. Lin YC, Chen MS, Zhong J (2008) Mater Lett 62:2136. doi:10.1016/j.matlet.2007.11.033
8. Lin YC, Chen MS, Zhong J (2008) Mech Res Commun 35:142. doi:10.1016/j.mechrescom.2007.10.002
9. Lin YC, Chen MS, Zhong J (2008) Comput Mater Sci 42:470. doi:10.1016/j.commatsci.2007.08.011
10. Rao KP, Prasad YKDV, Hawbolt EB (1998) J Mater Process Technol 77:166. doi:10.1016/S0924-0136(97)00414-7
11. Poliak EI, Jonas JJ (2004) ISIJ Int 44:1874. doi:10.2355/isijinternational.44.1874
12. Serajzadeh S (2008) Mater Sci Eng A 472:140. doi:10.1016/j.msea.2007.03.037
13. Capdevila C, Garcia-Mateo C, Caballero FG, García de Andrés C (2006) Comput Mater Sci 38:192. doi:10.1016/j.commatsci.2006.02.005
14. Perzyk M, Kochanski AW (2001) J Mater Process Technol 109:305. doi:10.1016/S0924-0136(00)00822-0
15. Altinkok N, Koker R (2005) J Mater Sci 40:1767. doi:10.1007/s10853-005-0689-5
16. Wang J, Van Der Wolk PJ, Van Der Zwaag S (2000) J Mater Sci 35:4393. doi:10.1023/A:1004865209116
17. Mandal S, Sivaprasad PV, Dube RK (2007) J Mater Sci 42:2724. doi:10.1007/s10853-006-1275-1
18. Kalaichelvi V, Sivakumar D, Karthikeyan R, Palanikumar K (2008) Mater Des. doi:10.1016/j.matdes.2008.06.022.
19. Garcia-Mateo C, Capdevila C, Caballero FG, García de Andrés C (2007) J Mater Sci 42:5391. doi:10.1007/s10853-006-0881-2
20. Lin YC, Zhang J, Zhong J (2008) Comput Mater Sci. doi:10.1016/j.commatsci.2008.01.039
21. Sun YB, Indacochea JE (1988) J Mater Sci 23:2339. doi:10.1007/BF01111885
22. Mittelstädt FG, Franco CV, Muzart J, de Souza AR, Cardoso LP (1996) J Mater Sci 31:431. doi:10.1007/BF01139161
23. Choi IS, Nam SW, Rie KT (1985) J Mater Sci 20:2446. doi:10.1007/BF00556073
24. Lee CK, Shih HC (2000) J Mater Sci 35:2361. doi:10.1023/A:1004772203501
25. Lin YC, Zhang J, Zhong J (2008) Comput Mater Sci. doi:10.1016/j.commatsci.2008.03.027
26. Lin YC, Zhang J, Zhong J (2008) Comput Mater Sci. doi:10.1016/j.commatsci.2008.03.010
27. Bhadeshia HKDH (1999) ISIJ Int 39:966. doi:10.2355/isijinternational.39.966